Journal of Geoscience and Environment Protection, 2025, 13(9), 289-314
https://www.scirp.org/journal/gep
ISSN Online: 2327-4344
ISSN Print: 2327-4336

Evaluating Geological Disaster Susceptibility Using Information Value and Neural Network Models: A Case Study of Xi Ao Town, Guangdong Province

Yinzhong Chen[1], Bo Tang[1*], Jinan Qiu[2], Aoyang Li[1]

[1]School of Resources and Planning, Guangzhou Xinhua University, Guangzhou, China
[2]Guangdong Geological Disaster Emergency Rescue Technology Center, Guangzhou, China
Email: tballen196@163.com

How to cite this paper: Chen, Y. Z., Tang, B., Qiu, J. N., & Li, A. Y. (2025). Evaluating Geological Disaster Susceptibility Using Information Value and Neural Network Models: A Case Study of Xi Ao Town, Guangdong Province. *Journal of Geoscience and Environment Protection, 13,* 289-314.
https://doi.org/10.4236/gep.2025.139014

Received: August 27, 2025
Accepted: September 27, 2025
Published: September 30, 2025

Abstract

Geological disaster susceptibility assessment provides a critical foundation for disaster prevention, mitigation, and formulation of governmental reduction policies and emergency management strategies, constituting a vital component of regional sustainable development. This study evaluated geological disaster susceptibility in the mountainous area of Xi Ao Town, northern Guangdong Province, China. We integrate the Information Value Model (IVM) with a Radial Basis Function Neural Network (RBF-NN) within a geographic information systems (GIS) framework. The assessment utilizes a comprehensive susceptibility evaluation system and field survey data of potential disaster sites to identify the key influencing factors and perform spatial zoning. The results indicate: 1) Geological disasters predominantly cluster on slopes with gradients of 55˚ - 75˚, sunny slopes, at elevations between 156.7 and 321.1 m, within lithological units dominated by Early Jurassic formations, within 100 m of fault zones, within 50 m of roads, 50 - 100 m of water systems, and within 50 m of residential areas. 2) Elevation, distance to residential areas, and slope gradient were the dominant factors influencing susceptibility within the study area. 3) The majority (85.39%) of the town's area was classified as low-susceptibility or non-susceptible. Medium-susceptibility zones accounted for 13.86% of the area, while high-susceptibility zones accounted for only 0.76%.

Keywords

Geohazard, Susceptibility, Informativeness Method, Artificial Neural Network, Xi Ao Town

1. Introduction

In recent years, global climate change, rapid urbanization, and the expanding scope of human activities have contributed to the increasing frequency and scale of geological disasters. These events pose serious threats to human safety and security. Research on geological disaster risk assessment has evolved into a relatively comprehensive theoretical system and methodological framework, encompassing disaster mechanisms, risk assessment models, regional evaluations, and practical applications. Theoretically, significant progress has been made in understanding the formation mechanisms of geological disasters, such as landslides, debris flows, and ground subsidence, providing a solid foundation for prediction and prevention efforts (Qi et al., 2012). Methodologically, technologies such as Remote Sensing (RS), Geographic Information Systems (GIS), and numerical simulations are widely employed for disaster monitoring and assessment. These tools enhance data acquisition and analysis efficiency, enabling the simulation of disaster processes to evaluate the extent of impact and damage severity (Su et al., 2025). Notably, the integration of big data and artificial intelligence (AI) technologies has further improved the accuracy of disaster prediction and assessment, offering a scientific basis for prevention and mitigation strategies (Bian et al., 2024). Research on geological disaster susceptibility dates to the 1970s. Dobrovolny pioneered spatial susceptibility zoning for landslides in the Anchorage area (Dobrovolny, 1964). Subsequently, Newman et al. conducted one of the first quantitative susceptibility assessments for the San Francisco area using computer technology (Newman et al., 1977). Building on theoretical foundations such as dynamical mechanism studies and environmental geohazard risk assessment (Ma et al., 2004; Li et al., 2008). Quantitative susceptibility evaluations and zoning research have advanced significantly. This progress involved establishing comprehensive disaster databases; collecting extensive geological, climatic, and hydrological data; and applying GIS and spatial analysis techniques (Nilsen & Brabb, 1973; Lee et al., 2000). As computer technology advanced and the capacity for processing multivariate information has improved, susceptibility assessment has evolved into a complex, multi-source nonlinear problem. This complexity has spurred the application of numerous advanced algorithms in this field (Gao, 2023). For instance, Pham et al. compared the performance of models such as logistic regression and Bayesian networks for landslide susceptibility assessments in Uttarakhand (Pham et al., 2016). Since the early 21st century, data-driven methods have gained increasing prominence in quantitative analysis (Zêzere et al., 2017). Machine learning (ML), as a key data-driven approach, offers advantages such as high accuracy, stability, and objectivity, helping minimize errors associated with human factors (Xiao et al., 2020). Artificial Neural Networks (ANNs) handle nonlinear, uncertain, and complex problems (Li et al., 2023). Alireza et al. achieved improved results in landslide hazard assessment using a novel hybrid model based on the Adaptive Neuro-Fuzzy Inference System (ANFIS) (Alireza et al., 2015). Similarly, Wu et al. applied Support Vector Machines (SVM) to predict landslide susceptibility along the Yangtze River banks in the Three Gorges Reservoir Area (Wu

et al., 2016). Shao et al. proposed a Sensitivity Coefficient Ratio (SCR) model based on the deterministic coefficient method for rainfall-induced landslides in Xuanhan City (Shao et al., 2018), and Guo et al. combined the weight-of-evidence method with a Back Propagation Neural Network (BPNN) for landslide susceptibility evaluation in Wanzhou District (Guo et al., 2019). The rapid development of computer technology and the advent of the "big data" era have provided new momentum for geological disaster risk prevention and control. Consequently, research paradigms that integrated artificial intelligence have become a prominent focus in the field.

In summary, researchers worldwide have achieved significant progress in geological disaster susceptibility evaluation, accumulating substantial practical experience and data resources in disaster risk investigation and assessment. However, these limitations will persist in the future. A deeper and comprehensive understanding of disaster-triggering factors and their inherent occurrence and development mechanisms is required. Opportunities exist to enhance methodological integration and application of new technologies. Key challenges include improving data accuracy and model reliability, strengthening interdisciplinary collaboration, and advancing the micro-scale refinement of susceptibility assessments. Therefore, continued scientific research on geological disaster susceptibility is crucial. It not only enhances the accurate identification and assessment of disaster risks but also provides a solid theoretical foundation and data support for formulating more scientific and effective prevention and control strategies, as well as emergency response plans. This research is vital for effectively safeguarding lives, properties, and societal stability.

Guangdong Province, characterized by extensive hilly and mountainous terrain, experiences frequent extreme weather events, notably heavy rainfall and typhoons. Significant topographic relief, complex geological structures, and intense rainfall erosion further increase its vulnerability. Compounding these natural factors, intensive human engineering activities have substantially increased both the susceptibility and frequency of geological disasters, posing severe threats to lives and infrastructure (Tang et al., 2024). To advance the provincial goals of "green development" and "ecological civilization construction", conducting rigorous geological disaster susceptibility assessments and predictions in Guangdong's mountainous regions is imperative. Developing robust susceptibility models and predicting disaster probabilities are essential for enhancing forecasting capabilities, elevating disaster prevention and mitigation efforts, effectively reducing geological risks, safeguard lives and property, and minimizing economic losses. This study has significant practical implications for disaster emergency response, safety engineering, and sustainable economic development in Guangdong.

Therefore, this study focused on Xi Ao Town, a representative mountainous area in northern Guangdong. By statistically analyzing field survey data of geological disaster risk sites and hidden hazards, integrated with GIS spatial analysis, we determined the types and spatial distribution patterns of disasters in Xi Ao. We then employed an integrated approach combining the Information Value Model (IVM) and a Radial Basis Function Neural Network (RBF-NN) to investigate the key influenc-

ing factors and spatial heterogeneity of geological disaster susceptibility. This work is critical for reducing geological disaster losses in northern Guangdong's mountains, improving regional disaster risk assessment management systems, supporting the strategic objectives of the Guangdong Millions Project, and ultimately providing enhanced geological safety assurance for the province's high-quality development.

2. Study Area and Data Sources

2.1. Study Area

Xi Ao Town is situated in the northernmost part of Longchuan County in Heyuan City, Guangdong Province, China. Belonging to the mountainous region of northern Guangdong, it lies approximately 106 km northwest of Longchuan County's administrative center. The town encompasses a jurisdictional area of 143 km^2 (Figure 1). The terrain is characterized by medium-low mountains with significant relief and steep slope gradients. Xi Ao experiences a typical subtropical monsoon climate, featuring concentrated heavy precipitation during the summer months. With the town comprising 12 villages and one neighborhood committee, supporting a population of approximately 23,000 residents. In recent decades

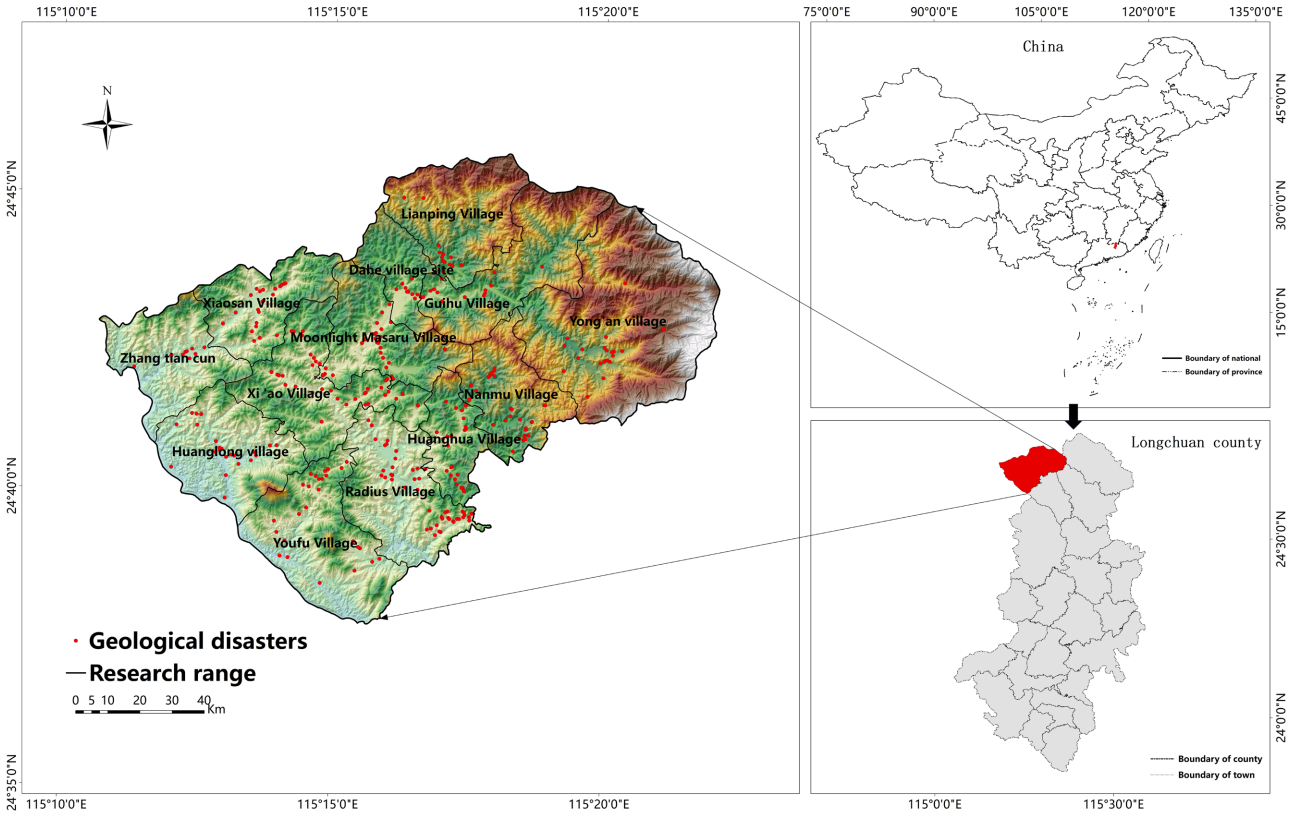

Figure 1. Study area.[1]

[1]Source of Figures 1-9 and Figure 14: Reprinted background map from the National Catalogue Service for Geographic Information (https://www.webmap.cn/main.do?method=index) under a CC BY license, with permission from the Ministry of Natural Resources of China, original copyright 2020.

extensive slope cutting for housing construction has significantly increased susceptibility to geological disaster. This vulnerability was first demonstrated in 2022 when heavy rainfall across Longchuan County triggered numerous landslides, flash floods, and debris flows. Xi Ao Town was among the most severely affected townships during this event.

2.2. Data Sources

This study primarily utilized data from *geologic hazard risk assessment* and *geologic hazard investigation and evaluation* projects conducted by the Guangdong Provincial Geological Hazard Prevention and Control Technology Center. The core dataset was obtianed from the 2022 Geological Hazard Fine Investigation Project in Longchuan County, Heyuan City, Guangdong Province. This included comprehensive field survey data and relevant historical records. Data for the known and hidden hazard points were extracted from this investigation. To ensure positional accuracy and research rigor, the geographical coordinates of all actual risk and hidden hazard points were verified and reprocessed using Global Positioning System (GPS) technology. The evaluation system incorporated key susceptibility influencing factors, including elevation, slope gradient, slope aspect, lithology, distance to faults, distance to roads, distance to rivers, distance to residential areas. Specific datasets for these factors were obtained from publicly available resources provided by the Guangdong Provincial Geological Environment Monitoring Station (http://dzj.gd.gov.cn/dzzhfzjszx/).

3. Methods

3.1. Evaluation System of Geological Hazard Susceptibility

The occurrence of geological disasters is characterized by suddenness, rapidity, and uncertainty and involves numerous influencing factors. These factors can be broadly categorized into two groups: internal factors (primarily topography, geological structure, engineering rock properties, and slope structure) and external factors (notably triggering agents such as rainfall and human activity) (Jiao et al., 2022). Based on comprehensive analysis of geological hazard development conditions specific to Xi Ao Town and adhering to the indicator selection guidelines outlined in the "*Technical Requirements for Informatization of Geological Hazard Investigation and Evaluation of Geological Hazard Risks in Towns and Streets of Guangdong Province (1:10,000)*", this study selected the following eight evaluation indices for geological hazard susceptibility: slope, slope direction, elevation, stratigraphic lithology, distance from fracture zones, distance from roads, distance from water systems, distance from residential areas as the evaluation indexes of geologic hazard susceptibility. These factors comprehensively represent the primary internal predisposing conditions and key external anthropogenic triggers relevant to Xi Ao. **Table 1** lists the specific data sources, and the classification schemes used for each index. The spatial distribution of these eight susceptibility indicators across the study area are shown in **Figures 2-9**.

Table 1. Geological hazard susceptibility evaluation index system of Xi Ao Town.

Number	Primary indicator (unit)	Secondary Indicators
1	Slope/˚	<15
		15 - 35
		35 - 55
		55 - 75
		>75
2	Slope direction	flat slope
		Shady slope
		Semi-Shady Slope
		Sunny slope
		Semi-sunny slope
3	Elevation /m	156.7 - 321.1
		321.1 - 454.2
		454.2 - 609.6
		609.6 - 813.8
		813.8 - 1293.4
4	Stratigraphic lithology	Early Cretaceous
		Early Jurassic
		Middle Jurassic
		Late Jurassic
		Early Aurignacian
		Late Aurignacian
5	Distance from fracture zones/m	<100
		100 - 200
		200 - 300
		300 - 500
		>500
6	Distance from roads/m	<50
		50 - 100
		100 - 150
		150 - 200
		>200
7	Distance from water systems/m	<50
		50 - 100
		100 - 150
		150 - 200
		>200

Continued

8	Distance from residential areas/m	<50
		50 - 100
		100 - 200
		200 - 500
		>500

1) Slope

The slope gradient critically controls the occurrence and evolution of geological hazards by governing the stability and kinematic potential of the surface materials. Steeper slopes experience amplified gravitational stresses, increasing susceptibility to the destabilization of rock and soil masses. This frequently causes landslides, rockfalls, and related hazards. Concurrently, steep gradients accelerate surface runoff velocity, intensify hydraulic erosion and compromise slope integrity. These slopes typically feature reduced vegetation coverage and diminished soil water retention capacity. Rapid saturation occurs under intense rainfall, significantly elevating risks of landslides and debris flows.

2) Slope direction

The slope aspect (direction) induces differential solar exposure, which significantly alters the physical properties of rock and soil, thereby modulating slope stability and hazard potential (Yu et al., 2023). South-facing (sunny) slopes exhibit heightened hazard susceptibility compared to north-facing (shady) slopes owing to distinct microclimatic effects: enhanced convective activity promotes orographic precipitation, increasing hydrological triggers for mass movements; pronounced diurnal thermal fluctuations accelerate physical weathering, reducing rock cohesion; persistent drying-rewetting cycles degrade material integrity through expansive stresses. These mechanisms collectively increase the failure probability on sun-exposed slopes.

3) Elevation

Elevation exerts multi-scale controls on hazard genesis by integrating topographic, pedogenic, and ecological influences. As a primary descriptor of terrain configuration (mountain ranges, valleys, and plains), it correlates strongly with weathering intensity and regolith thickness, groundwater dynamics, soil moisture regimes, vegetation communities, and land-use patterns (Xie et al., 2023). In Xi Ao Town, elevations range from 156.79 m to 1,293.24 m (**Figure 7**). These data were classified into five discrete intervals using zonal statistics and the Jenks Natural Breaks algorithm, optimizing within-group homogeneity for susceptibility modeling.

4) Stratigraphic lithology

Stratigraphic lithology fundamentally controls slope stability through its physical and mechanical properties (Wu et al., 2016). The rock composition and structure dictate weathering susceptibility, strength anisotropy, and stress redistribution. These properties determine the failure modes: massive igneous rocks favor

planar sliding, whereas unconsolidated sediments enable debris flow. Xi Ao's Early Jurassic formations (predominantly sandstones interbedded with shales) exhibit pronounced differential weathering that is conducive to instability.

5) Distance from fracture zones

Regions with frequent development of tectonic activities imply an unusually active process of accumulation and release of internal stresses in the Earth's crust, a phenomenon that greatly alters the stability of the geological structure. In such a region, the strong mechanical effects of mutual extrusion, tension or shear of crustal plates lead to significant deformation of the surface and underground rock layers, forming a series of complex geotectonic forms such as fracture zones and folded mountain ranges. These tectonic zones are characterized by tectonic stress concentration, rock fragmentation and active crustal movement, which make the physical and mechanical properties of rocks fragile and weaken the shear strength, thus greatly increasing the probability of occurrence of the geologic disasters (Wu et al., 2021). According to the buffer zone analysis, the geological tectonic buffer distance of Xi Ao Town was divided into five categories, as shown in **Figure 6**.

6) Distance from roads

Xi Ao Town is in the low hills of northern Guangdong; the villages are mainly distributed in rivers and valleys, and the house buildings are generally built adjacent to the mountains. During the construction of roads in mountainous areas, excavation of mountain slopes frequently occurs, which directly affects the original stability of mountain slopes, increases the risk of geological disasters, and lurks in landslides, collapses, and other safety hazards (Wang et al., 2020). In the process of road construction and operation, the disturbing effect on the slope land on both sides of the road may destroy the balance and stability of the slope soil body, thus inducing geological disasters. According to the distance from the roads, the road slope is affected by different degrees, and the road buffer distance in Xi Ao Town was divided into five categories, as shown in **Figure 7**.

7) Distance from water system

The cutting effect of rivers and gullies creates suitable spatial conditions for the occurrence of geological hazards and becomes the main occurrence of geological hazards. The cutting depth and density of rivers and gullies in Hoshi Au Town significantly affect the distribution density of geological hazards. The slopes on both sides of the river are subject to the river's infiltration, scouring and side erosion all year round, which weakens the friction between the soil bodies, anti-slip ability declines, and cracks are formed; thus, that soil body loses its support, destroys the balance and triggers geological disasters (Li et al., 2022). The closer the water system is to the slope, the greater the influence on the stability of the slope, and the more likely geological disasters will occur.

8) Distance from the residential area

The study area is a low mountainous and hilly area in northern Guangdong. Villages in mountainous areas are mainly distributed along rivers and valleys, and houses are mostly built on the mountains. Unreasonable excavation or slope

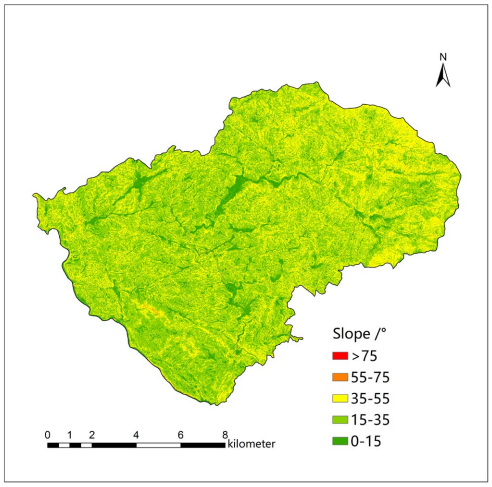

Figure 2. Slope.

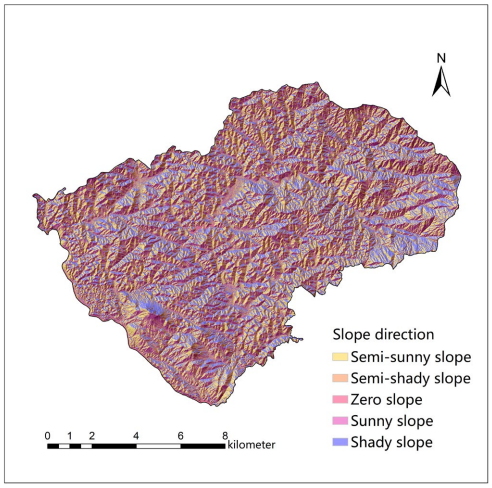

Figure 3. Slope direction.

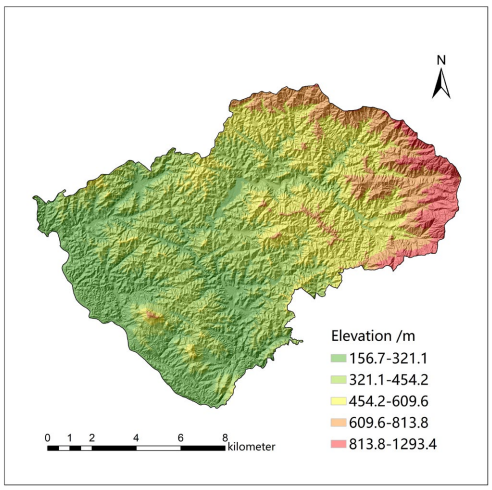

Figure 4. Elevation.

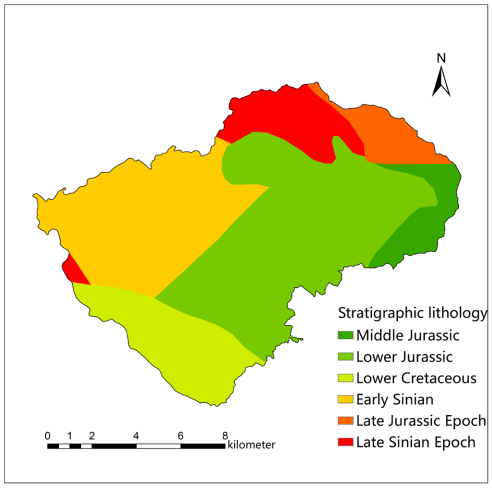

Figure 5. Stratigraphic lithology.

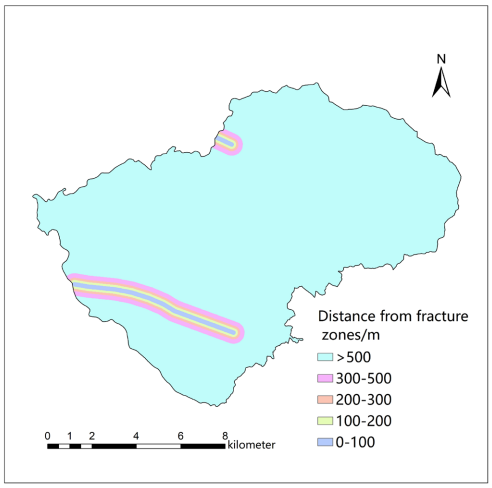

Figure 6. Distance from fracture zones.

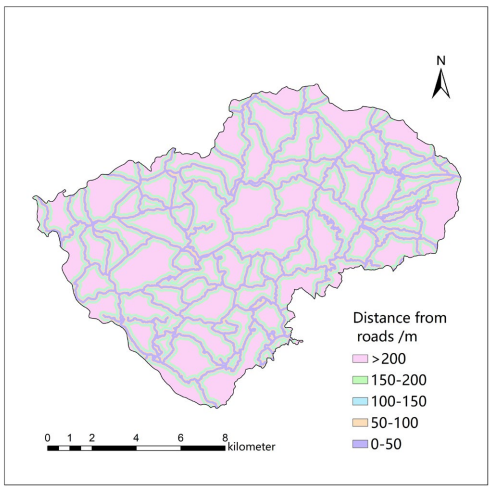

Figure 7. Distance from roads.

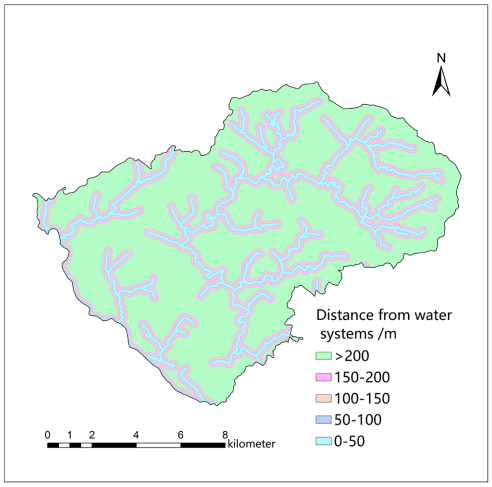

Figure 8. Distance from water systems.

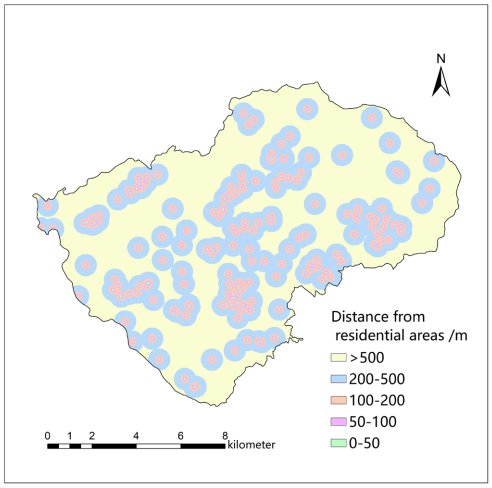

Figure 9. Distance from residential areas.

cutting at the foot of mountain slopes leads to the loss of the original stability of the soil body of mountain slopes, which creates favorable conditions for the occurrence of geologic hazards. The degree of influence on geological hazards also varies. depending on the distance from the settlement.

3.2. IVM

IVM is a statistical method, based on the Bayesian probability model, which is mainly based on the informativeness of the influencing factors to quantitatively measure the relevance of each influencing factor to the research object (Ruan & Huang 2001). According to the classification results of each evaluation index, the number of raster and the number of geological hazards in different classification states of each evaluation index were counted using the GIS software, and the information quantity value of each evaluation index in Xi Ao Town was calculated by applying formula (1), and then the value of each evaluation index was assigned.

$$I = \sum_{i=1}^{n} I(\chi_i, H) = \sum_{i=1}^{n} \ln \frac{N_i/N}{S_i/S} \quad (1)$$

I denotes the value of informativeness, which is mainly used to reflect the possibility of destruction of evaluation cells; n represents the number of indicators, H denotes the number of risk points and hidden dangers, S denotes the number of grid cells. N denotes the total number of evaluation cells that have undergone deformation and destruction; Si denotes the number of grid cells of indicator x_i, N_i denotes the number of indicators x_i that have suffered from environmental geohazards number of grid cells. When $I > 0$, the greater the amount of information, the greater the probability that geological disasters may occur; when $I < 0$, it indicates that the indicator is unfavorable to the occurrence of geological disasters; when $I = 0$, it indicates that there is no connection between the indicator and the occurrence of geological disasters, that is, the indicator cannot be adopted as an indicator for the comprehensive evaluation of the susceptibility to geological disasters in Xi Ao town (Zhu et al., 2021).

3.3. RBF-NN

Artificial Neural Networks (ANNs) are highly nonlinear, ultra-large-scale continuous-time dynamical systems formed by extensively interconnected processing units (neurons) (Shao et al., 2011). ANNs employ a multilayer structure incorporating bias and negative feedback mechanisms, with training systems involving both positive and negative feedback processes. During the positive feedback phase of network training, the input data are processed by the hidden layer and transmitted from the input layer to the output layer to generate preliminary prediction results. These outputs were then compared with the expected target values. When deviations occurred, the system activated a negative feedback mechanism. At this stage, the errors propagated backward along the network path. Through iterative adjustment of inter-neuronal weight coefficients, discrepancies between predictions and targets are progressively reduced or eliminated. This process continuously optimizes network performance until predetermined requirements are met. In this study, we applied neural network analysis to partition geological hazard susceptibility results for Xi Ao Town. Our network model (**Figure 10**) comprises input, hidden, and output layers with full interlayer connectivity. Network training was achieved through continuous adjustment of weights and thresholds (Guo et al., 2000).

RBF-NN is a special three-layer structure (**Figure 11**): the input layer is responsible for receiving external input signals, and consists of multiple source points or perceptual units, which convert the data of the actual problem into a form that can be processed by the network; the hidden layer adopts RBF, and this layer performs the very important nonlinear mapping function, which transforms the data points in the input space into a new implied feature space ; the output layer is linear, and based on the result of the nonlinear transformation of the hidden layer, it directly responds to the input patterns after linear combination, which leads to

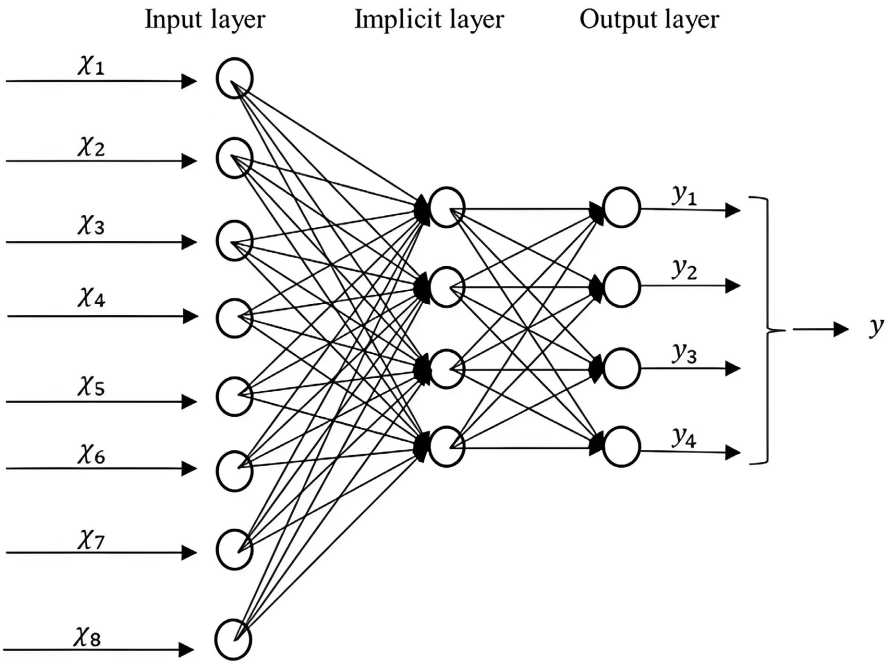

Figure 10. Schematic diagram of neural network operation.

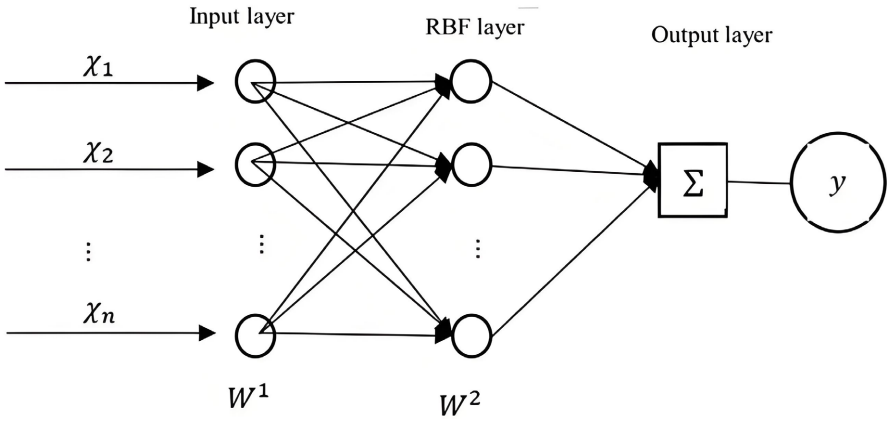

Figure 11. Structure of RBF-NN.

the final network output (Gu, 2013). Its input/output relationship can be described by the following equation (2):

$$\begin{cases} u_i = \exp\left[-\dfrac{\|X - c_i\|}{2\sigma_i^2}\right] \\ y = \sum_{i=1}^{n} w_{ij} u_i - \theta \end{cases} \quad i = 1, 2, \cdots, n;\ j = 1, 2, \cdots, n \tag{2}$$

$X = (x1, x2, ..., xn)$ denotes the input data; c_i denotes the central value of the function; σ_i denotes the constant required for the study, which determines the distance of the base function to the central value; n denotes the number of neurons in the hidden layer of the network model; w_{ij} denotes the weight of neuron i in the hidden layer of the network model linking neuron j in the output layer of the network model; θ denotes the output layer of the network model neuron critical

value; y denotes the output content of the network model.

The learning process of the RBF-NN corresponds to the training process, involving inputting training data into the network model for autonomous learning. Key characteristics of this model include its capacity for self-optimizing parameters, thereby reducing manual parameter adjustment workload and lowering research costs. This capability enables the network model to achieve enhanced performance across diverse datasets and experimental tasks. Simultaneously, it reduces zoning errors introduced by human parameter adjustments during the partitioning of geological hazard susceptibility evaluation results, while improving partitioning efficiency.

4. Analysis of Results

4.1. Selection of Evaluation Unit

In the process of geohazard evaluation research and practice, the evaluation unit is defined as the smallest unit for geohazard susceptibility evaluation, which is the spatial carrier of geohazard danger, vulnerability, susceptibility and risk measurement, and the basis for the implementation of disaster prevention and mitigation measures and planning and management. Whether the selection and division of the evaluation unit is reasonable is crucial to the relevance, scientific natural and operability of the evaluation results. Currently commonly used evaluation units can be regular shapes, such as grid cells or grid cells divided into certain sizes, or shapes of different sizes, such as slope units, watershed units or regional units (Gao et al., 2006). Considering that this study area is characterized by a small range and small amount of data, the grid cell was selected as the basic evaluation unit to evaluate susceptibility. The grid cells were in accordance with the accuracy requirements, and the size of the grid was calculated with reference to the empirical formula (Xue et al., 2018):

$$G_s = 7.49 + 0.0006s - 2\times10^{-9}\times s^2 + 2.9\times10^{-15}\times s^3 \quad (3)$$

s is the scale of the map of the study area, i.e., 1:10,000, which is calculated to be $G_s = 13.3$, and thus the size of the grid is determined to be 12.5 m × 12.5 m.

4.2. Influencing Factors of Geological Disaster Susceptibility

First, it is necessary to quantify all evaluation indicators and then input them into the network model in the form of numerical values for calculation. Only the data after quantitative processing can be inputted and calculated by the network model; therefore, it is necessary to quantify all evaluation indicators (He, 2014). To comprehensively and accurately assess the geohazard susceptibility of each evaluation unit, it is necessary to consider the specific state of each influencing factor within the unit and its interaction relationship, and to calculate the comprehensive information quantity under the combined situation of various evaluation factors (Zhu et al., 2021). The information quantity method was used to analyze and obtain the information quantity calculation results of eight geological hazard sus-

ceptibility indicators in Xi Ao Town and assign their values (Table 2).

Table 2. Evaluation factor information and assignment statistics.

Serial number	Evaluation Factor	Evaluation Level	Informativeness value	Assignment
1	Slope/˚	<15	0.54	3
		15 - 35	−0.78	1
		35 - 55	0.14	2
		55 - 75	3.42	4
		>75	0	/
2	Slope direction	Flat slope	0	/
		Shady slope	−0.86	1
		Semi-Shady Slope	−0.07	2
		Sunny slope	0.48	4
		Semi-sunny slope	−0.07	3
3	Elevation/m	156.7 - 321.1	0.59	4
		321.1 - 454.2	0.24	3
		454.2 - 609.6	−0.97	2
		609.6 - 813.8	−3.49	1
		813.8 - 1293.4	0	/
4	Stratigraphic lithology	Early Cretaceous	−0.44	2
		Early Jurassic	0.44	4
		Middle Jurassic	0	/
		Late Jurassic	0	/
		Early Aurignacian	0.06	3
		Late Aurignacian	−2.61	1
5	Distance from fracture zones/m	<100	0.86	5
		100 - 200	0.13	4
		200 - 300	−1.3	1
		300 - 500	−0.24	2
		>500	0	3
6	Distance from roads/m	<50	1.28	5
		50 - 100	0.4	4
		100 - 150	−0.73	3
		150 - 200	−0.81	2
		>200	−2.23	1
7	Distance from water systems/m	<50	0.79	4
		50 - 100	1.24	5
		100 - 150	0.3	3
		150 - 200	−0.34	2
		>200	−0.73	1

Continued

8	Distance from residential areas/m	<50	2.45	5
		50 - 100	1.49	4
		100 - 200	1.36	3
		200 - 500	0.07	2
		>500	−1.76	1

According to the spatial distribution pattern and informativeness analysis of each indicator in the evaluation index system, the eight selected influencing factors were causally related to susceptibility to geological disasters in Xi Ao Town. According to the 300 geological disaster hidden spots collected in Xi Ao Town, the information value was calculated, and the indicators were graded using the equal spacing or natural breakpoint method to determine the magnitude of the influence of each evaluation indicator and sub-interval on the geological disaster. The information value and variance of the information value of the evaluation indicators of geological disaster susceptibility in Xi Ao Town are shown in Table 3.

Table 3. Informative value and variance of each evaluation indicator.

Number	Evaluation Factor	Number of disasters site	Evaluation level	Informativeness value	Informativeness Variance
1	Slope/˚	64	<15	0.54	2.083933
		70	15 - 35	−0.78	
		126	35 - 55	0.14	
		40	55 - 75	3.42	
		0	>75	0.00	
2	Slope direction	0	Flat slope	0.00	0.183049
		29	Shady slope	−0.86	
		59	Semi-Shady Slope	−0.07	
		135	Sunny slope	0.48	
		77	Semi-sunny slope	−0.07	
3	Elevation/m	139	156.7 - 321.1	0.59	2.183874
		133	321.1 - 454.2	0.24	
		27	454.2 - 609.6	−0.97	
		1	609.6 - 813.8	−3.49	
		0	813.8 - 1293.4	0.00	
4	Stratigraphic lithology	26	Early Cretaceous	−0.44	0.077302
		186	Early Jurassic	0.44	
		0	Middle Jurassic	0.00	
		0	Late Jurassic	0.00	
		86	Early Aurignacian	0.06	
		2	Late Aurignacian	−2.61	

Continued

5	Distance from fracture zones/m	8	<100	0.86	0.485441
		4	100 - 200	0.13	
		1	200 - 300	−1.30	
		6	300 - 500	−0.24	
		281	>500	0.00	
6	Distance from roads/m	185	<50	1.28	1.412685
		67	50 - 100	0.40	
		19	100 - 150	−0.73	
		15	150 - 200	−0.81	
		14	>200	−2.23	
7	Distance from water systems/m	62	<50	0.79	0.515097
		92	50 - 100	1.24	
		34	100 - 150	0.30	
		17	150 - 200	−0.34	
		95	>200	−0.73	
8	Distance from residential areas/m	31	<50	2.45	2.113243
		34	50 - 100	1.49	
		99	100 - 200	1.36	
		108	200 - 500	0.07	
		28	>500	−1.76	

Table 4. Cumulative contribution of evaluation indicators.

Number	Evaluation Factor	Informativeness Variance	Indicator contribution	Cumulative contribution
1	Elevation/m	2.183874017	0.241189	24.12%
2	Distance from the residential area /m	2.113242532	0.233388	47.46%
3	Slope/°	2.083932551	0.230151	70.47%
4	Distance to road/m	1.412685006	0.156018	86.07%
5	Distance to water system/m	0.515096699	0.056888	91.76%
6	Distance to fracture zone/m	0.485441293	0.053613	97.12%
7	Slope direction	0.183048906	0.020216	99.15%
8	Stratigraphic lithology	0.077302392	0.008537	100.00%

By analyzing the informativeness values, the susceptibility to geological hazards in Xi Ao Town was found to be most influenced by four factors: distance from settlements, distance from roads, elevation and slope. Based on the variance of the informativeness values, it can be concluded that the four indicators of distance from settlements, elevation, slope, and distance from roads play a significant role in influencing susceptibility to geological hazards in Xi Ao Township. Finally, the

ratio of the informativeness variance of the eight evaluation indicators of Xi Ao town to the total informativeness variance was used to indicate the contribution of each evaluation indicator in the evaluation of the susceptibility to geological hazards in Xi Ao town: the higher the contribution, the higher the influence of the indicator on the degree of occurrence of geological hazards. As shown in **Table 4**, the three indicators of elevation, distance from settlements and slope had a greater influence on the degree of geological disaster occurrence, and stratigraphic lithology had the least influence.

4.3. Geological Disaster Susceptibility Zoning

The geological disaster susceptibility zoning assessment was conducted by integrating the informativeness Method and the ANN Model. As the ANN model requires prior training before application, the evaluation process is divided into two parts: 1) training the neural network model and 2) susceptibility assessment and zoning (Gao et al., 2006).

1) Neural Network Model Training

Training the neural network model serves as a foundational step in geological disaster susceptibility assessment. Parameter optimization is a prerequisite to ensure model reliability, which can be achieved either through standalone calibration procedures or integrated with susceptibility zoning workflows. The optimization process involves five critical stages: Construction of optimization indicator layers: Integrate geospatial parameters derived from the Information Value Model (IVM); Grid-based spatial discretization: Divide the study area into 12.5 × 12.5 m resolution grids using GIS; Data extraction: Compile training datasets from historical disaster inventories and environmental variables; Data standardization: Normalize input variables (mean = 0, SD = 1) to eliminate dimensional heterogeneity; Model optimization: Implement a hybrid genetic algorithm-backpropagation approach to minimize prediction errors.

2) Susceptibility zone

Following model validation, the optimized ANN is deployed for susceptibility zoning through a parallelizable workflow: indicator layer development: establish multi-criteria evaluation layers; grid system implementation: maintain spatial consistency with the training phase using identical grid specifications; predictor variable extraction: execute batch processing of spatial data through Python-GIS interfaces; data normalization: apply min-max scaling to ensure comparability across heterogeneous parameters; susceptibility classification: generate probabilistic susceptibility maps (0 - 1 scale) and classify zones using quantile thresholds.

4.3.1. Neural Network Model Training

After getting the quantized training data, use the RBF neural network object created in MATLAB and set up the training parameters, then call the function to train the model, after setting up the training parameters, you can point to "start training" (Dong et al., 2024). The simulation training of the RBF neural network model used in this study is the process of calling functions that have been inte-

grated into the neural network toolbox of the MATLAB software (Figure 12). The length of this simulation training is closely related to the size of the data volume of the input training samples and the settings of the parameters before training, especially the number of neuron increments, the maximum number of neurons allowed, the error of the neural network, and the expansion speed of the model have a greater impact. The input training sample data in this study accounted for 1% of the total data volume of Xi Ao Town, that is, 973 grid cells.

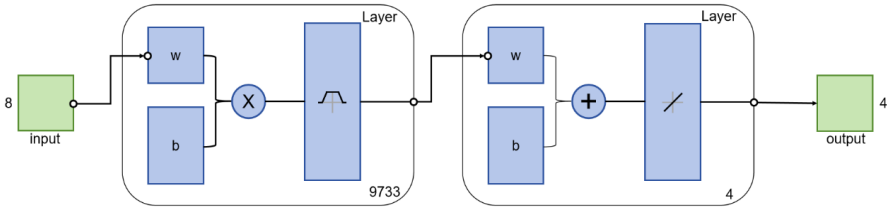

Figure 12. Schematic operation of neural network structure.

The spread of the newrbe function of the RBF-NN model has a close relationship with its training accuracy, and it needs to be repeatedly debugged until the model operation results reach the optimization in the actual running process of the model. The debugging of the model operation needs to be set according to a certain rule of different sizes of the expansion speed to obtain the optimal training data, the expansion speed of the model operation is generally in the range of 0.2 - 5, and the value of the expansion speed is the number of the first term of the isotropic series with the first term of 0.2 and the common difference of 0.2. At the end of the model training, the training error control and the training accuracy analysis graph (Figure 13) were made by comparing the written down values of the spreading with the corresponding values of the training accuracy.

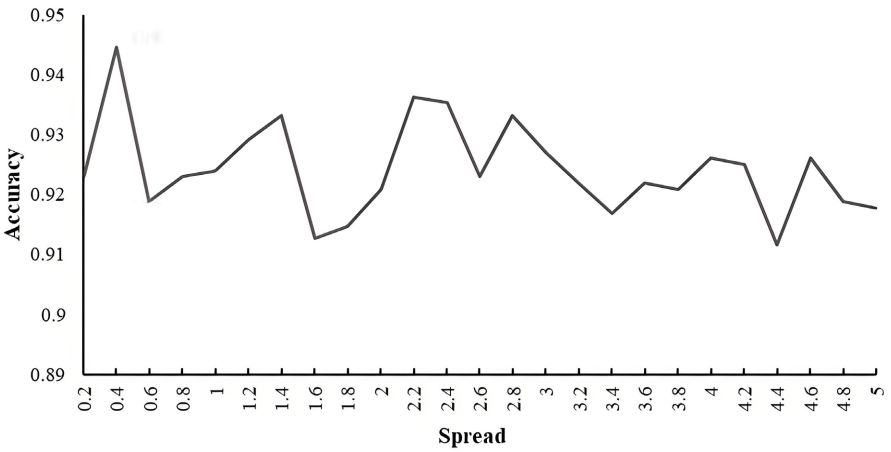

Figure 13. Expansion speed and accuracy.

By analyzing the table corresponding to the model expansion speed value and training accuracy, it is concluded that only when the expansion speed of the neural network model is 0.4, the accuracy of the neural network model training is the

highest and at the peak. Therefore, in this study, the neural network model expansion speed of 0.4 was selected as the final parameter of training to complete the training of the network model. After the training of the neural network model was completed, the index data of Xi Ao Town, which is similar to Xi Ao Town in terms of natural environment, and the finalized parameters of the neural network model were used to carry out the evaluation of the susceptibility of Xi Ao Town to geologic hazards and partitioning, and finally, the results of the evaluation were superimposed on the registered historical geologic hazard sites to verify the accuracy of the neural network model.

4.3.2. Susceptibility Zoning

Partitioning of the geohazard susceptibility evaluation results constitutes the final stage of the assessment. This process involves two key components: model computation and conversion of the evaluation results into spatial layers. Using the trained RBF-NN model and processed index data, we implemented MATLAB's integrated RBF-NN function to calculate and output susceptibility values for Xi Ao Town. These numerical outputs directly correspond to susceptibility levels according to Guangdong Province's "*Technical Requirements for Informatization of Geological Disaster Risk Survey and Evaluation (1:10,000) in Townships (Streets) (Trial Implementation)*". Xi Ao Town is classified as high susceptibility, medium susceptibility, low susceptibility, and non-susceptibility, and the corresponding output result values were 4, 3, 2, and 1. The output result values were obtained through the calculation of the RBF-NN model and were imported into the GIS for the calculation of the output results and imported into the GIS for conversion to derive the geohazard susceptibility zoning results of Xi Ao Town (Table 5, Figure 14).

Table 5. The results of susceptibility zoning

Zoning	Area (m^2)	%	Geohazard sites
Non-susceptibility	1312944.792	0.87%	2
Low susceptibility	128096655.5	84.52%	37
Medium susceptibility	21004221.29	13.86%	165
High susceptibility	1144893.69	0.76%	96

1) High susceptibility zone

The high susceptibility area of geological hazards in Xi Ao Town covers 1.14 square kilometers (0.76% of the township's area), primarily distributed in the northern part of Guihu Village and the northern/southeastern parts of Yongan Village within high-altitude hilly areas. These areas feature elevation above 321.1 meters, slopes of 55˚ - 75˚, and sunny/semi-sunny aspects. Vulnerable to collapse and rockfall disasters when affected by Guangdong's "Dragon Boat Water" continuous rainfall and typhoon events.

2) Medium-susceptibility zone

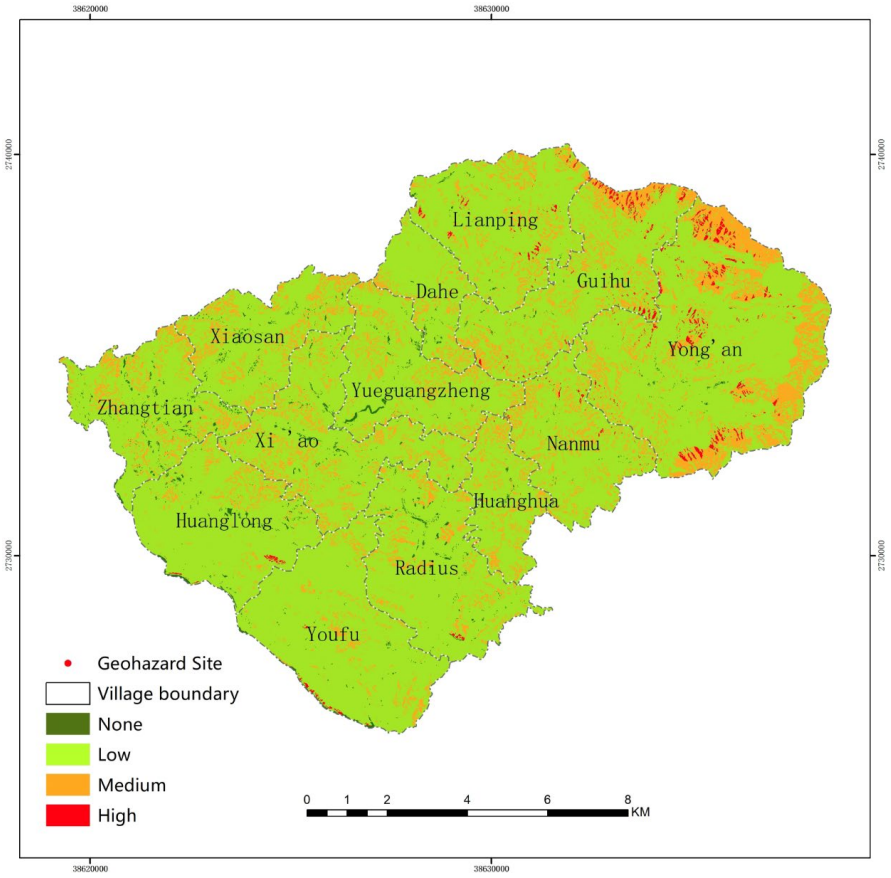

Figure 14. Geologic Hazard Susceptibility Zoning of Xi Ao Town.

Medium susceptibility areas cover 13.86% of Xi Ao Town, widely distributed across mid-low altitude gentle slopes (156.6 - 321.1m elevation, ≤15˚ slopes, semi-sunny aspects) within 50 - 100 m of roads and 50m of rivers. These zones accumulate slope toe materials and require preventive monitoring against hazards triggered by heavy rainfall.

3) Low susceptibility zone

Low susceptibility zones account for 84.52% of the township, mainly occurring at lower elevations with moderate slopes, shady aspects, and significant distances from roads/rivers. A geologically stable environment presents minimal risk but necessitates continuous stability monitoring for early warning.

4) Non-susceptibility zone

Non-susceptibility areas (0.87% of townships) occur in remote locations far from settlements/rivers/roads with minimal human impact and stable geological conditions, serving as designated safe zones and hazard avoidance sites.

5. Discussion

Geohazard vulnerability assessment serves not only as a technical instrument but also as a critical bridge connecting natural science with sustainable development objectives. This micro-scale study of geohazard susceptibility in Xi Ao Town,

Longchuan County, employs classical statistical methodologies combined with neural network modelling to enhance evaluation precision. Spatial prediction of geological hazards represents an inherently interdisciplinary endeavor that integrates geoscience, engineering geology, geographic information systems, remote sensing technology, and computer science. Notwithstanding these advances, this study has limitations that require further investigation; the exclusive use of RBF-NN for susceptibility modeling warrants comparison with alternative neural architectures (e.g., BP, SOM, and CNN) to assess their applicability and relative efficacy in geohazard contexts. Concurrently, the accuracy of RBF-NN training requires refinement through advanced optimization techniques. 1% of the training data is insufficient and may not represent the complete distribution of the entire dataset, which to some extent affects accuracy. Future research should incorporate multi-source data fusion (high-resolution remote sensing, InSAR deformation monitoring) with ensemble machine learning approaches (Random Forest, Deep Learning) to elevate spatial prediction reliability. Finally, in the actual management of geologic disasters, there is a close relationship between disaster prevention and control and the identification of disaster risk points and hidden dangers, and the management of geologic disasters is an important link to ensure the safety of human life and property, and it also plays a vital role in the prevention and control of geologic disasters. As an important area for geological hazard research in northern Guangdong, the natural geographical environment and human activities are the main reasons for the susceptibility of geological hazards in mountainous areas. Elevation, distance to residential areas, and slope as the most influential factors, the monitoring of changes in terrain environment and the control of human engineering construction have become the main directions and challenges for the prevention and control of geological disasters in mountainous areas. The monitoring of changes in terrain environment and the control of human engineering construction have become the main directions and challenges for the prevention and control of geological disasters in mountainous areas. The monitoring of changes in terrain environment and the control of human engineering construction have become the main directions and challenges for the prevention and control of geological disasters in mountainous areas. Therefore, in the future, it is necessary to strengthen the work related to the management of geologic disaster prevention and control, and further strengthen the collection, processing and analysis of information on geologic disaster risk zones and hidden danger points and strengthen the synchronous monitoring with the information on geologic disaster prevention and control.

6. Conclusion

This study analyzed the geological disaster mechanisms and formation conditions in Xi Ao Town, a high-incidence area in northern Guangdong Province, by collecting fundamental geological data and historical disaster records. Eight key susceptibility factors were identified in the present study. Using ArcGIS spatial anal-

ysis tools, we stratified the evaluation indexes while applying the information value model to link the influence factor layers with historical disaster data and calculated the information values for each factor level. The RBF neural network model comprehensively evaluated Xi Ao Town's geological disaster susceptibility and generated susceptibility zone results. There are several main conclusions as follows:

1) Terrain slope 55˚ - 75˚, terrain slope toward sunny slope, elevation 156.7 - 321.1 m, stratigraphic lithology dominated by the Early Jurassic, 100 m near the fracture zone, within 50 m of the road, within 50 - 100 m of the water system, within 50 m of the settlement are the concentrated areas of Xi Ao Township where geological hazards occur.

2) Based on the informativeness value calculated by overlaying the number of geological hazards and factor layers in Xi Ao Township based on the informativeness model, and then quantitatively processing each evaluation index, we summarized that elevation, distance from the settlements, and terrain slope were the main reasons for the frequent occurrence of geological hazards in Xi Ao Township.

3) By analyzing the susceptibility zoning of Xi Ao Township, it was found that most of the areas in Xi Ao Township have low susceptibility and non-susceptibility zones, accounting for 85.39% of the township's area, a few areas are medium susceptibility zones accounting for 13.86% of the township's area, and a very small number of areas are high susceptibility zones accounting for 0.76% of the township's area.

Acknowledgements

This study was supported by the Department of Forecasting and Networking, China Meteorological Administration (Grant No. FPZJ2025-128, FPZJ2025-129).

Data availability statement

The original contributions presented in the study are included in the article/Supplementary material, further inquiries can be directed to the corresponding authors.

Authors' Contributions

BT: Data curation, Funding acquisition, Methodology, Project administration, Writing—review and editing. YC: Conceptualization, Data curation, Investigation, Methodology, Software, Writing—original draft. JQ: Investigation, Methodology, Resources, Writing—review and editing. AL: Methodology, Resources, Writing—review.

Funding

The author(s) declared that financial support was received for the research, authorship, and/or publication of this article. We are grateful for the financial support from project of the Philosophy and Social Science Planning Project of Guangdong Prov-

ince (Number: GD24XGL035); Guangdong General Colleges and Universities Characteristic and Innovative Projects (Number: 2024KTSCX126); College students' innovative entrepreneurial training program (Number: 202413902003); Teaching Reform Project of Guangzhou Xinhua College (Number: 2023KCJ001).

Conflict of interest

The authors declare that the research was conducted in the absence of any commercial or financial relationships that could be construed as a potential conflict of interest.

References

Alireza, D., Nasiri, I., Biswajeet, A. et al. (2015). A New Hybrid Model Using Step-Wise Weight Assessment Ratio Analysis (SWARA) Technique and Adaptive Neuro-Fuzzy Inference System (ANFIS) for Regional Landslide Hazard Assessment in Iran. *Catena, 135,* 122-148.

Bian, Y., Chen, H., Liu, Z., Chen, L., Guo, Y., & Yang, Y. (2024). Geological Disaster Susceptibility Evaluation Using Machine Learning: A Case Study of the Atal Tunnel in Tibetan Plateau. *Sustainability, 16,* Article 4604. https://doi.org/10.3390/su16114604

Dobrovolny, E. (1964). *Landslide Susceptibility in and near Anchorage as Interpreted from Topographic and Geologic Maps*.

Dong, L., Liu, Y., Huang, J., & Liu, H. L. (2024). An Early Prediction Model of Regional Landslide Disasters in Fujian Province Based on Convolutional Neural Network. *Hydrogeology and Engineering Geology, 51,* 145-153.

Gao, K., Cui, P., Zhao, C., & Wei, F. Q. (2006). Landslide Hazard Evaluation of Wanzhou Based on GIS Information Value Method in the Three Gorges Reservoir. *Chinese Journal of Rock Mechanics and Engineering, 5,* 991-996.

Gao, R. (2023). *Research on Regional Debris Flow Susceptibility Assessment Based on Machine Learning Methods*. Jilin University.

Gu, L. (2013). Data Sparse Issue of Collaborative Filtering Algorithm Based on GEP-RBF. *Computer and Digital Engineering, 41,* 1433-1436.

Guo, Z., Chen, Z., Song, B., Zhang, X. L., & Fang, Z. (2000). Applied Momentum BP Algorithm to Predict Groundwater Level. *Journal of East China Normal University (Natural Science), 3,* 79-84.

Guo, Z., Yin, K., Fu, S., Huang, F. M., Gui, L., & Xia, H. (2019). Landslide Susceptibility Assessment Based on GIS and WOE-BP Model. *Earth Science, 44,* 4299-4312.

He, Z. (2014). *Design and Implementation of Geological Hazard Information System Based on Neural Network Evaluation Model*. Master's Thesis, University of Electronic Science and Technology of China.

Jiao, W., Zhang, M., Xie, X., Li, C. W., Liu, T., & Pang, S. (2022). Evaluation of Urban Geological Hazard Susceptibility Based on GIS and Weighted Information Value Model: A Case Study of Daxin. *Safety and Environmental Engineering, 29,* 119-128.

Lee, S., Ryu, J., Choi, W., & Won, J. (2000). Development and Application of Landslide Susceptibility Analysis Techniques Using Geographic Information System. In *IEEE 2000 International Geoscience and Remote Sensing Symposium. Taking the Pulse of the Planet: The Role of Remote Sensing in Managing the Environment. Proceedings (Cat. No.00CH37120)* (pp. 319-321). IEEE. https://doi.org/10.1109/igarss.2000.860505

Li, X., Li, S., Chen, J., & Liao, Q. (2008). Coupling Effect Mechanism of Endogenic and Exogenic Geological Processes of Geological Hazards Evolution. *Chinese Journal of Rock Mechanics and Engineering, 27,* 1792-1806.

Li, X., Ruan, M., Yang, F., Liu, C. Z., & Yang, Y. P. (2022). Evaluation of Geological Hazard Susceptibility Based on GIS and Information Method: A Case Study of Changjiang County, Hainan Province. *Geology and Resources, 31,* 98-105.

Li, Z., Pan, C., & Wu, Y. (2023). Application Status and Prospects of Artificial Neural Networks in Prediction. *Sci-Tech Innovation and Productivity, 44,* 27-30.

Ma, Y., Zhang, Y., Zhang, C., Wang, J. (2004). Theory and Approaches to the Risk Evaluation of Geological Hazards. *Journal of Geomechanics, 10,* 7-18.

Newman, E. B., Paradis, A. R., & Brabb, E. E. (1977). *Feasibility and Cost of Using a Computer to Prepare Landslide Susceptibility Maps of the San Francisco Bay Region, California*. U.S. Department of the Interior.

Nilsen, T., & Brabb, E. (1973). Current Slope Stability Studies by the U.S. Geological Survey in the San Francisco Bay Region, California. *Publication of Landslide, 1,* 2-10.

Pham, B. T., Pradhan, B., Bui, D. T., Prakash, I., & Dholakia, M. B. (2016). A Comparative Study of Different Machine Learning Methods for Landslide Susceptibility Assessment: A Case Study of Uttarakhand Area (India). *Environmental Modelling & Software, 84,* 240-250.

Qi, X., Tang, C., Chen, Z., & Shao, C. (2012). Research on Geological Hazard Risk Assessment. *Journal of Natural Disasters, 21,* 33-40.

Ruan, S., & Huang, R. (2001). Application of GIS-Based Information Model on Assessment of Ecological Hazards Risk. *Journal of Chengdu University of Technology (Science & Technology Edition), 1,* 89-92.

Shao, D., Zhang, X., & Wu, D. (2011). Study on the Prediction of Average Ecological Footprint of Suzhou Based on BP Neural Network Model. *Territory & Natural Resources Study, 2,* 47-48.

Shao, S., Tang, M., Nie, B., Li, Y., Wang, F. L., & Yang, H. (2018). Spatial Distribution Patterns and Susceptibility Analysis of Rainfall-Induced Landslides in Xuanhan Area. *Journal of Yangtze River Scientific Research Institute, 35,* 41-46+51.

Su, B., Zhang, J., Tang, Y., Yu, J., Wang, E., Vashishtha, G., & Li, Z. (2025). Geological Disaster Detection in Underground Mining Tunnels Using a New Electromagnetic Method: Theoretical Modeling and Experimental Evaluation. *Journal of Applied Geophysics, 233,* Article 105641.

Tang, B., Ren, H., Qiu, J. A., Miao, C., & Chen, Y. (2024). Evaluation of Geo-Hazard Risks in the Pearl River Delta Based on Geographic Information System and Weighted Informativeness Approach. *Frontiers in Environmental Science, 12,* Article 1406386.

Wang, L., Wu, J., Zhao, B., Yao, Z. Q., & Zhang, L. Q. (2020). Susceptibility Assessment of Geohazards in Chizhou City of Anhui Province Based on GIS and Informative Model. *The Chinese Journal of Geological Hazard and Control, 31,* 96-103.

Wu, J., Jiang, S., Wu, Q., Li, H. L., & Qiu, E. (2021). Landslide Geological Hazard Vulnerability Evaluation Based on GIS and BP Neural Network. *Resources Environment & Engineering, 36,* 100-104+107.

Wu, X., Shen, S., & Niu, R. (2016). Landslide Susceptibility Prediction Using PSO-SVM Model Supported by GIS. *Geomatics and Information Science of Wuhan University, 41,* 665-671.

Xiao, T., Segoni, S., Chen, L., Yin, K., & Casagli, N. (2020). A Step Beyond Landslide Susceptibility Maps: A Simple Method to Investigate and Explain the Different Outcomes

Obtained by Different Approaches. *Landslides, 17,* 627-640. https://doi.org/10.1007/s10346-019-01299-0

Xie, S., Chen, S., Chen, J., Wang, J., & Tao, F. (2023). Susceptibility Evaluation of Mountain Environmental Geological Disasters Based on GIS and Information Model: Taking Zigui County in Hubei Province as an Example. *Resources Environment & Engineering, 37,* 567-577.

Xue, K., Xiong, L., Zhu, S., & Tang, G. (2018). Extraction of Loess Dissected Saddle and Its Terrain Analysis by Using Digital Elevation Models. *Journal of Geo-Information Science, 20,* 1710-1720.

Yu, K., Wu, T., Wei, A., Wu, Y. P., Dai, F. G., & Liu, Y. (2023). Geological Hazard Assessment Based on the Models of AHP, Catastrophe Theory and Their Combination: A Case Study in Pingshan County of Hebei Province. *The Chinese Journal of Geological Hazard and Control, 34,* 146-155.

Zêzere, J. L., Pereira, S., Melo, R., Oliveira, S. C., & Garcia, R. A. C. (2017). Mapping Landslide Susceptibility Using Data-Driven Methods. *Science of the Total Environment, 589,* 250-267. https://doi.org/10.1016/j.scitotenv.2017.02.188

Zhu, W., Zou, H., He, M., & Wang, J. (2021) Research on Geological Disaster Susceptibility Division Method Based on BP Neural Network. *Resources Environment & Engineering, 35,* 840-844. https://doi.org/10.16536/j.cnki.issn.1671-1211.2021.06.012